Journal of Materials Chemistry A

RSC Publishing

PAPER

View Article Online
View Journal | View Issue

Cite this: J. Mater. Chem. A, 2013, 1, 3932

Printable fabrication of Pt-and-ITO free counter electrodes for completely flexible quasi-solid dye-sensitized solar cells

Huawei Zhou, Yantao Shi,* Da Qin, Jiang An, Lingling Chu, Chaolei Wang, Yudi Wang, Wei Guo, Liang Wang and Tingli Ma*

Received 3rd November 2012
Accepted 10th January 2013

DOI: 10.1039/c3ta00960b

www.rsc.org/MaterialsA

Low-cost bendable photoanodes and counter electrodes (CEs), as well as gel electrolytes, are potentially desired for the mass production of completely flexible dye-sensitized solar cells (DSSCs). In this work, *via* printing at low temperature, we fabricated titanium carbide (TiC)-functionalized conductive-carbon (CC) on flexible polyimide (PI) films to replace traditional and expensive Pt/ITO/PEN CEs. Morphology characterization revealed this composite CE was highly porous and homogeneous. Electrochemical investigations demonstrated that this Pt-and-ITO free flexible CE exhibited a high electro-catalytic activity. Finally, the conversion efficiencies of the all flexible quasi-solid DSSCs using this low-cost TiC-CC/PI CE achieved 86% of that based on a Pt/CC/PI CE. Thus, the facile fabrication process of this novel CE, along with its notable performance, are quite promising for the future roll-to-roll production of completely flexible DSSCs.

1 Introduction

At the arrival of an energy crisis and global warming, how to utilize renewable energy effectively remains a hot topic worldwide for scientists. Dye-sensitized solar cells (DSSCs) have gained widespread scientific and technological interest, not only because they demonstrate specific advantages over traditional photovoltaic devices, but also because they can exhibit other superiorities such as environmental friendliness, low incident-light-angle dependence, colorization, *etc.*[1–3] Nowadays, more and more portable electronic devices are widely used, therefore, lightweight and flexible DSSC devices are ideal candidates to serve as their mobile power supply.[4–6]

Generally, DSSCs mainly consist of a photoanode, electrolyte and counter electrode (CE). For a flexible DSSCs device, bendable photoanodes and CEs are both necessary.[7] In recent years, some contributions have been reported to fabricate flexible CEs using tin oxide coated polyethylene naphthalate (ITO-PEN) film and Pt as the conducting substrate and catalyst, respectively. For example, Wu *et al.* reported a flexible CE fabricated by introducing Pt into the carbon nanotube (CNT) matrix and then coating this catalyst layer onto the ITO/PEN substrate.[8] Although Pt-based flexible CEs have demonstrated better catalytic activity and performances, as we know, the high price of Pt will limit its future application in DSSCs. In the meantime, ITO accounts for approximately 60% of the total cost of DSSCs. Therefore, developing Pt-and-ITO free flexible CEs will be quite beneficial for cost reduction and thus largely promote the practical applications of DSSCs. According to previous reports, some Pt-and-ITO free CEs have been developed and applied in DSSCs, however, most of these DSSCs were actually not completely flexible devices, because in their fabrication the photoanodes were still fabricated on rigid glasses.[9,10] Thus, we could not estimate their actual performances in completely flexible DSSC devices. On the other hand, for mass production of flexible DSSCs devices, the roll-to-roll technique requires printable and viscous gel electrolytes. Up to now, there is no relevant report concentrating on a completely flexible, quasi-solid, Pt-and-ITO free DSSC system.

Recently, our group has developed a series of inorganic non-Pt catalysts for efficient CEs in DSSCs.[11] Among these low-cost catalysts, some exhibited a similar catalytic behaviour to Pt and also their performances in DSSCs were comparable to that of traditional Pt CEs. Fabrications of these non-Pt CEs on FTO glass have been published, however, all flexible DSSCs devices based on these promising CE materials have not been reported up to now. In this work, we report a rapid and facile, large scale and low-cost printing approach to prepare Pt-and-ITO free flexible counter electrodes on plastic substrates at low temperature. Conductive-carbon (CC) paste and TiC-functionalized CC paste were printed on the flexible polyimide (PI) substrate to fabricate the counter electrodes, named CC/PI and TiC-CC/PI, respectively. For comparison, another CE designated as Pt/CC/PI was prepared by coating Pt nanoparticles on CC/PI. Systematic characterizations focusing on the microstructures and catalytic activities of these three CEs were carried out in our

State Key Laboratory of Fine Chemicals, School of Chemical Engineering, Dalian University of Technology, Dalian, China. E-mail: tinglima@dlut.edu.cn; shiyantao@dlut.edu.cn; Fax: +86-411-84986230; Tel: +86-411-84986237

experiments. Results indicated that the highly porous TiC-CC/PI CE demonstrated a high electro-catalytic activity in the reduction of redox couples in the electrolyte. Finally, the TiC-CC/PI based completely flexible quasi-solid DSSCs exhibited a conversion efficiency of 4.26%, comparable to that based on a Pt/CC/PI CE.

2 Experimental section

2.1 Preparation of the three kinds of CE

CC/PI CE: the flexible PI film was coated with a low-cost commercial CC paste (Shenzhen DongDaLai Chemical Co., Ltd.) by a simple screen-printing technique. Then the CC-coated PI film was annealed consecutively at 150 °C for 30 min and at 250 °C for 30 min, respectively.

TiC-CC/PI CE: the TiC-CC paste was produced by mixing TiC and CC paste at a weight ratio of 1 : 1 and ball-milling for 1 h. CC in the TiC paste can significantly improve the adhesion between TiC and the conductive substrate, as well as the conductivity and stability of the TiC-CC/PI CE. The TiC-CC paste was then coated onto the as-prepared CC/PI by a screen-printing technique. The films were then dried and sintered at 250 °C for 30 min.

Pt/CC/PI: the preparation of the Pt-coated flexible electrode using Triton X-100 dispersed Pt nanoparticles suspension was conducted as follows: CC/PI was immersed into the solution containing 4% conditioner (ML-371, Rockwood Electrochemical Asia, Ltd.) with ultrasonic processing at room temperature for 5 min. The conditioner did not only attach itself onto the CC/PI but also varied the surface charge state for adsorption of other particles or ions. After the conditioned CC/PI was rinsed with deionizer water, the film was immediately immersed in the Triton X-100 Pt suspension for 5 min. The as-prepared flexible CE was again rinsed with deionizer water and then dried at 100 °C.

2.2 Preparation of the gel-type polymer electrolyte

The new gel-type polymer electrolyte for DSSCs was obtained by immersing the poly(vinyl alcohol-*co*-methyl methacrylate) copolymers into the I_3^-/I^- based liquid electrolyte with stirring for 24 h. The liquid electrolyte contained 0.1 M lithium iodide, 0.6 M 1-propyl-3-methyl-imidazolium iodide, 0.05 M I_2, 0.1 M guanidine thioisocyanate, 0.5 M 4-*tert*-butylpyridine and methoxypropionitrile solvent.

2.3 Preparation of the flexible TiO_2 photoelectrodes at low temperature and flexible DSSCs device fabrication

The flexible TiO_2 photoelectrode was produced by coating low-temperature binder-free P25 TiO_2 paste (75% anatase and 25% rutile, with an average primary particle size of 21 nm and a specific surface area of 55 m^2g^{-1}, Evonik/Degussa) on the ITO/PEN plastic substrate *via* the doctor-blade technique. To further improve the properties of mechanical strength and light scattering, we added the second bifunctional (VK-TA100) layer (anatase, with an average particle size of 150 nm). Then the raw film was sintered at 120 °C for 0.5 h. After cooling down to about 80 °C, the photoelectrode was immersed in 0.5 mM solution of N719 in ethyl alcohol for 20 h. Finally, the flexible DSSCs were assembled by sandwiching the gel-type polymer electrolyte with a photoanode and CE. The active area of our DSSCs devices for the photocurrent–voltage (*J–V*) test was 0.16 cm^2.

2.4 Characterization and measurements

The square resistances and film thickness of our CEs were measured using a four-point probe measurement system (RST-9, China) and step profiler (Surfcom 130A, Japan), respectively. Then, the morphologies of our three CEs were characterized using a scanning electron microscope (SEM) (FEI, NOVA NanoSEM 450) and *J–V* curves of their corresponding flexible DSSCs measured under AM 1.5 and 100 mW cm^{-2} illumination with a Keithley digital source meter (2601, USA) equipped with a solar simulator (PEC-L15, Peccell, Yokohama, Japan). For electrochemical impedance spectra (EIS) and Tafel characterizations, the dummy cell was assembled using two identical flexible CEs filled with our gel-type polymer electrolytes and sealed by the double-faced insulated adhesive spacer. Note that this architecture was similar to our DSSCs and the active area of the dummy cell was 0.49 cm^2. The dummy cells were measured in the dark with a computer-controlled electrochemical workstation (Zennium Zahner, Germany). In the meantime, Tafel curves were obtained with another workstation (CHI630, Chenhua, Shanghai), by which Cyclic voltammetry (CV) was conducted at a scan rate of 10 mV s^{-1} in a three-electrode system, as reported in our previous work.[12]

3 Results and discussion

3.1 Morphologies and electro-catalytic activities of the three kinds of CE

Morphologies of the three CEs were well illustrated by scanning electron microscope (SEM) images in Fig. 1. As we can see from Fig. 1(a) and (b), the particles in the as-prepared CC/PI exhibited a wide size distribution, from several nanometers to microns. When composited with TiC by a ball-milling process, Fig. 1(c) and (d) show a highly porous and homogeneous morphology for the TiC-CC/PI CE. This desired nanostructure in the TiC-CC/PI CE can offer a large surface area for catalytic reactions and meanwhile largely improve the mechanical contact between the TiC-CC and substrate. For flexible DSSC devices, strength of the mechanical contact is extremely important since it is expected that the active layers on the plastic substrates will not be destructed after frequent bending in practical applications. Also it should be mentioned that CC in the composite paste played important roles in improving the adhesion and conductivity. Our approach to fabricate this novel Pt-and-ITO free CE is well suited to the fabrication of flexible CEs and future industrial production. For our reference Pt/CC/PI CE, there was no ball-milling in the fabrication process, and Fig. 1(e) reveals that the morphologies of the carbon particles remained almost the same as that in Fig. 1(a). On the other hand, obviously, these Pt nanoparticles were loaded on the surface of the carbon particles (see Fig. 1(f)).

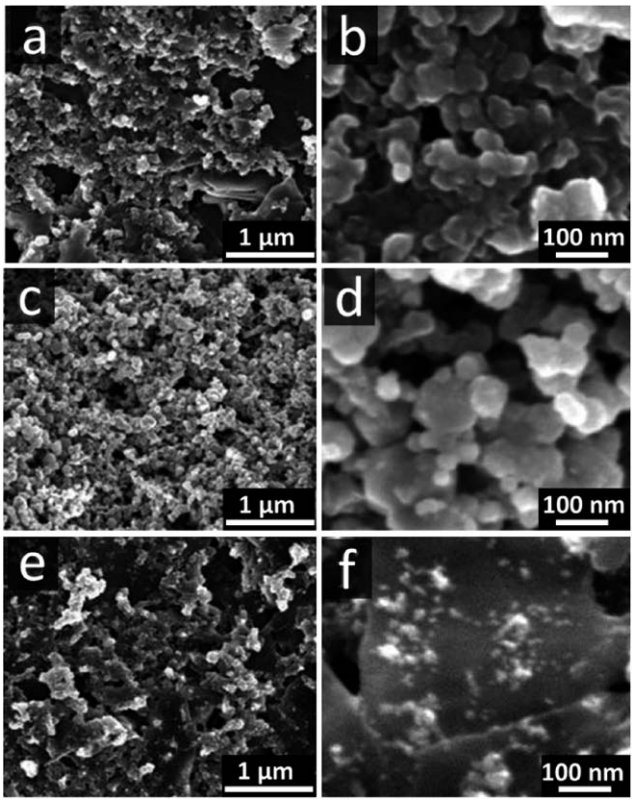

Fig. 1 SEM images of the three kinds of flexible CE: (a) CC/PI; (c) TiC-CC/PI; (e) Pt/CC/PI; and (b, d and f) are the high magnification images for CC/PI, TiC-CC/PI and Pt/CC/PI, respectively.

To characterize the catalytic activities of the CC/PI, TiC-CC/PI and Pt/CC/PI CEs, cyclic voltammetry (CV) experiments were performed. Two consecutive pairs of redox peaks in the cyclic voltammogram for the two-electron transfer process of iodide species were used in this study. The relative negative pair with a significant effect on the DSSCs performance can be assigned to the redox reaction represented by eqn (1), whereas the positive pair was assigned to the redox reaction represented by eqn (2).[13]

$$I_3^- + 2e^- = 3I^- \quad (1)$$

$$3I_2 + 2e^- = 2I_3^- \quad (2)$$

As shown in Fig. 2, a cathodic peak of the CC electrode at a relatively negative potential is absent. According to the reaction of eqn (1), this result shows that the electro-catalytic activity of the CC/PI electrode for the reduction reaction of triiodide ions is extremely slow under our experimental conditions involving a low concentration of triiodide ions ($[I^-]/[I_2] = 10:1$) in liquid electrolyte. After being composited with TiC, it can be easily observed that the desired reduction behaviour became obvious according to the CV curve of the TiC-CC/PI. Also, the CV curve of TiC-CC/PI is very similar to that of Pt/CC/PI, illuminating that TiC-CC/PI has similar electro-catalytic functions for the redox reaction to the Pt/CC/PI electrode. This result further confirms that TiC may demonstrate a similar electronic structure to that of the noble metals. Therefore, it can be said that the introduction of TiC brings about improvements of the electro-catalytic performance of Ti-CC/PI.

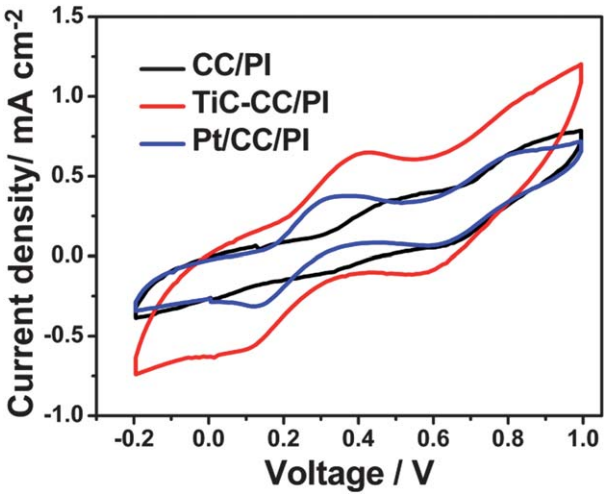

Fig. 2 Cyclic voltammograms of the three kinds of CE.

On the other hand, from Fig. 2 we can also find that TiC-CC/PI has a larger peak current than that of Pt/CC/PI. As we know, the peak current in the CV curve is determined by the following equation:

$$I_P = (2.69 \times 10^5) n^{3/2} C D^{1/2} A v^{1/2} \quad (3)$$

Where n is the number of electrons transferred in each redox reaction (in this case, $n = 2$), C is the concentration, D is the diffusion coefficient, v is the potential scan rate and A is the active area of the electrode. Thus, according to the slope of the Randles–Sevcik eqn (3),[14] we can easily infer that the TiC-CC/PI CEs have a larger active surface area, in good accordance with the SEM obtained.

3.2 Photovoltaic performance and electrochemical investigations of the flexible quasi-solid DSSCs

For future roll-to-roll production of completely flexible devices, we chose the polymer gel electrolyte and flexible photoanode to fabricate our quasi-solid DSSCs. Fig. 3 shows the photocurrent density–voltage (J–V) curves of these DSSCs based on CC/PI, TiC-CC/PI and Pt/CC/PI CEs. Detailed photovoltaic parameters are summarized in Table 1. Firstly, the DSSCs based on CC/PI CE exhibit poor values of both fill factor (FF) and power conversion efficiency (PCE), only 0.40 and 2.02%, respectively. The FF was mainly affected by resistance of the cell and catalytic activity of the CE. When using the TiC-CC/PI CEs, remarkable photovoltaic improvements were achieved, presenting a FF and PCE of 0.68 and 4.26%, respectively. Except for FF, the increases in short-circuit current density (J_{sc}) and open-circuit voltage (V_{oc}) are also contributions to the photovoltaic improvements. In this view, it is thought that the efficient catalytic activity of TiC-CC/PI is validated for polymer gel electrolytes in DSSCs. As a comparison, the DSSCs based on Pt/CC/PI CEs demonstrate a higher PCE of 4.92%. Also worth highlighting is that the PCE of

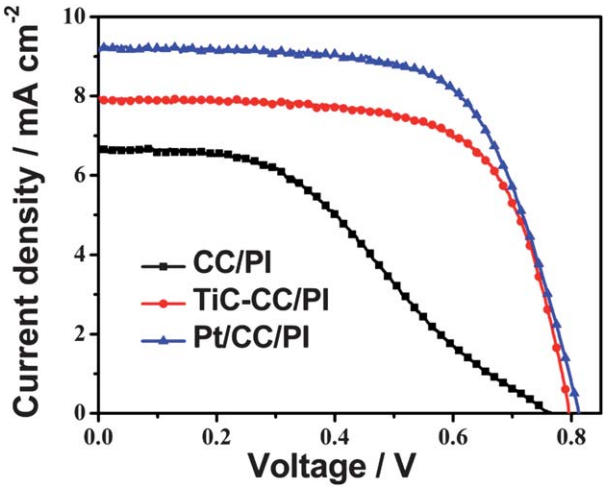

Fig. 3 Photocurrent density–photovoltage (*J–V*) curves for the DSSCs using three kinds of CEs.

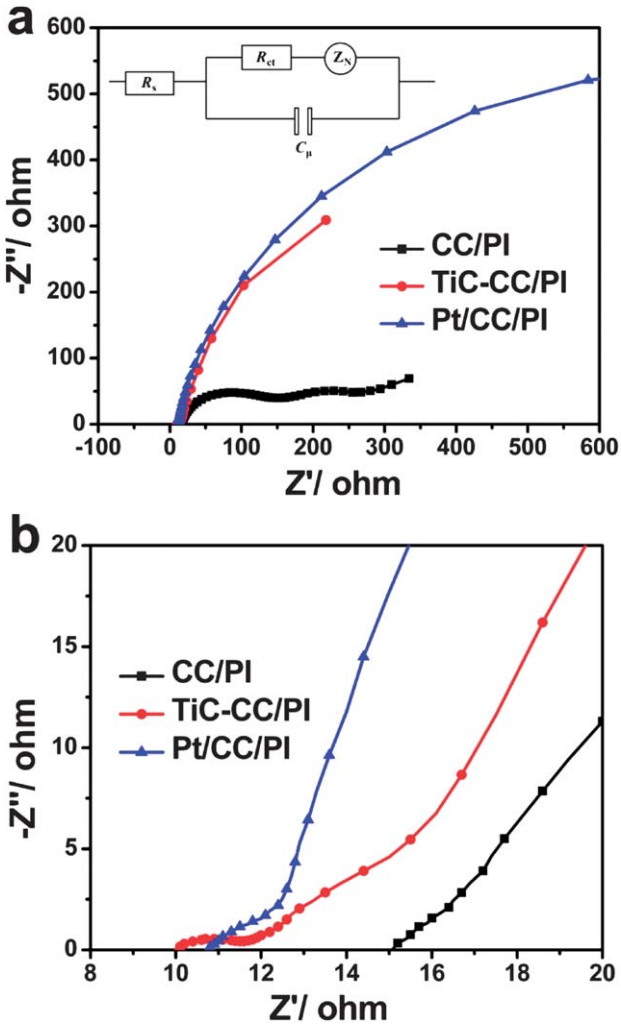

Fig. 4 (a) Nyquist plots of the symmetrical cells based on the three kinds of CE; the inset shows the corresponding equivalent circuit diagram and (b) an enlarged view of higher frequencies in Nyquist plots of the dummy cell based on the three kinds of CE.

the DSSCs using TiC-CC/PI CEs have reached 86% of the photovoltaic performance of the DSSCs with a Pt/CC/PI CE. In conclusion, the photovoltaic performances are enough to highlight the predominant synergistic effect of CC and TiC in the CEs.

For better understanding of the catalytic activity of the three kinds of CEs for our polymer gel electrolyte, electrochemical impedance spectroscopy (EIS) and Tafel-polarization measurements were carried out. In EIS characterization, symmetric dummy cells were assembled by sandwiching the polymer gel electrolyte with two identical CEs. The Nyquist plots of these three flexible CEs based symmetric dummy cells are shown in Fig. 4. In addition, the inset of Fig. 4a shows an equivalent circuit diagram used to fit the spectra with the 'Z-View' non-linear least-squares fitting program.[15] Typically, the intercept on the real axis is assigned to the series resistance (R_s) describing the ohmic resistance of the load and the conducting substrates. The charge transfer resistance (R_{ct}) can be obtained by fitting the arc observed at higher frequencies in Nyquist plots (left most semicircle) to the equivalent circuit shown in the inset of Fig. 4. Low-frequency regions (right semicircle) arise from the Nernst diffusion impedance (Z_N) of the triiodide–iodide couple in the gel-type polymer electrolyte.

The sheet resistance of the CEs together with other parameters obtained by fitting Nyquist plots are summarized in Table 1, from which the R_s value of CC/PI is found to be slightly larger than that of TiC-CC/PI or Pt/CC/PI. For the CEs, what we care about most is the charge transfer resistance R_{ct}. We can find from Table 1 that the CE of CC/PI has a quite large R_{ct} value, indicating a poor catalytic activity for the carbon material in our experiment. In addition, its diffusion resistance impedance Z_N is also more obvious when compared with the other two CEs. This can be attributed to the slow ionic diffusion in the porous structure of CC/PI. Although film morphologies have some effect on the devices performances', here, it is clear that higher R_s, R_{ct} and Z_N for CC/PI are responsible for the poor FF and J_{sc} of the corresponding DSSCs, listed in Table 1. Subsequently, introduction of TiC or Pt into the CC-based system can bring about obviously reduced R_{ct} for the TiC-CC/PI and Pt/CC/PI, in good accordance with the CV characterizations. The above

Table 1 Photovoltaic parameters of the DSSCs using three kinds of flexible CEs and EIS parameters of the dummy cells based on these electrodes

CE	Thickness μm^{-1}	V_{oc} V^{-1}	J_{sc}/mA cm^{-2}	FF	PCE/%	□/Ω sq^{-1}	R_s Ω^{-1}	R_{ct} Ω^{-1}	Z_N Ω^{-1}
CC/PI	15	0.76	6.66	0.40	2.02	4.35	15.16	147.00	514.6
TiC-CC/PI	23	0.80	7.93	0.68	4.26	4.60	10.29	1.67	83.2
Pt/CC/PI	15	0.81	9.21	0.66	4.92	4.30	10.81	3.94	101.2

results confirm again the importance of the TiC or Pt in the catalytic reduction in DSSCs. On the other hand, the Z_N values of the polymer gel electrolytes in the TiC-CC/PI and Pt/CC/PI are much lower than that in CC/PI, implying the ionic diffusion in the gel electrolyte is highly related to the pore structure or catalytic activity of the CE, the detailed reasons are still under investigation.

To further analyze the interfacial charge transfer processes between polymer gel electrolytes and these three different CEs, Tafel curve plots were obtained in a dummy cell similar to the one used in the EIS experiments. As shown in Fig. 5, log J is a function of the potential (U). Typically, the Tafel curve consists of three zones.[16] The curve at the very high potential corresponds to the limiting diffusion zone, which is related to the transport of triiodide and iodide in the electrolyte. Then, the middle potential range (with a sharp decrease) can be attributed to the Tafel zone, where the current density of charge transfer appears. Finally, the curve at a low potential ($|U| < 120$ mV) is attributed to the polarization zone. Through comparing the current density in the Tafel zone in Fig. 5, the CC/PI CE exhibits much slower charge transfer processes, in agreement with its EIS and J–V results in DSSCs. However, the TiC-CC/PI curve shows a large slope as well, as does that of Pt/CC/PI, which indicates that the TiC-CC/PI CE has a high catalytic activity for polymer gel electrolytes. The limiting current density (J_{lim}) at a very high potential depends on the diffusion of the triiodide–iodide redox couple in the DSSCs system. Also, the result of J_{lim} for these three CEs is in good accordance with that of Z_N derived from EIS characterization. Finally, we can find that the axis of symmetry of the Tafel curve of CC/PI and TiC-CC/PI CEs are all deviated from the centre of voltage axis. These behaviours may have strong connections with the pore-filling process of the polymer gel electrolyte into the porous CEs.

Developing printable TCO and Pt-free CEs is very important for large scale and low-cost DSSCs in the future. As we know, the screen-printing technique is the most facile for rapid and large-scale fabrication of electrodes for DSSCs, with different active areas and patterns. In our experiment, CC paste has a high viscosity, a prerequisite for screen-printing. Then, better conductivity of the CC paste is quite necessary for substitution of the ITO substrate for fast electron transport. Besides, the cost of TiC powder and CC paste is undoubtedly affordable. Finally, the high-temperature annealing procedure above 250 °C is not needed for the fabrication of the TiC-CC/PI CE. Hence, it is concluded that our approach is facile, low-cost and rapid for the mass-production of flexible CEs.

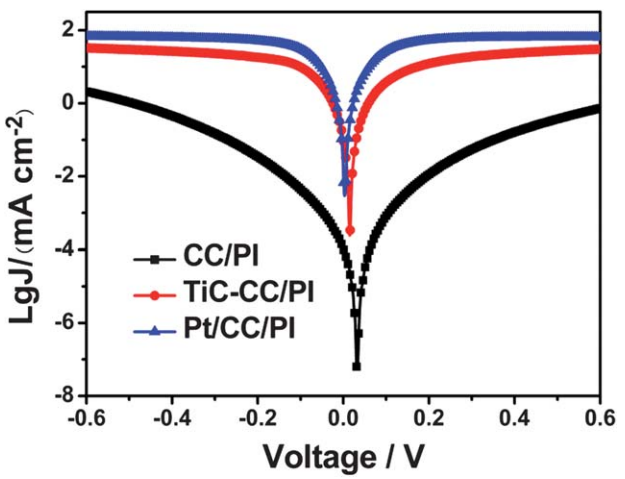

Fig. 5 Tafel curves of the symmetrical cells based on the three kinds of CE.

4 Conclusions

In summary, at low temperature we successfully developed a low cost and facile approach to fabricate a TiC functionalized carbon CE on a plastic PI substrate. It has been proven that TiC is compatible with CC for the formation of highly porous and homogeneous structures and the introduction of TiC could also obviously improve the electro-catalytic activity. Finally, the conversion efficiencies of our all flexible quasi-solid DSSCs using this TiC-CC/PI CE achieved 86% of that of flexible DSSCs based on a Pt/CC/PI CE. The whole procedure is eco-friendly and commercially viable, in addition, it will be promising for the future mass-production of completely flexible DSSCs by the roll-to-roll technique.

Acknowledgements

This work was financially supported by NSFCs (Grant no. 51273032), National High Technology Research and Development Program for Advanced Materials of China (Grant no. 2009AA03Z220), Specialized Research Fund for the Doctoral Program of Higher Education of China (20110041110003), Open project of the State Key Laboratory for Physical Chemistry of Solid Surfaces of Xiamen University (Grant no. 201210) and the State Key Laboratory of Fine Chemicals of Dalian University of Technology.

Notes and references

1 B. Oregan and M. Gratzel, *Nature*, 1991, **353**, 737–740.
2 A. Yella, H.-W. Lee, H. N. Tsao, C. Yi, A. K. Chandiran, M. K. Nazeeruddin, E. W.-G. Diau, C.-Y. Yeh, S. M. Zakeeruddin and M. Graetzel, *Science*, 2011, **334**, 629–634.
3 I. Chung, B. Lee, J. He, R. P. H. Chang and M. G. Kanatzidis, *Nature*, 2012, **485**, 486–U494.
4 S. A. Haque, E. Palomares, H. M. Upadhyaya, L. Otley, R. J. Potter, A. B. Holmes and J. R. Durrant, *Chem. Commun.*, 2003, 3008–3009.
5 S. S. Kim, J. H. Yum and Y. E. Sung, *J. Photochem. Photobiol., A*, 2005, **171**, 269–273.
6 L. Yang, G. Xin, L. Q. Wu and T. L. Ma, *Process. Chem.*, 2009, **21**, 2242–2249.
7 X. O. Yin, Z. S. Xue and B. Liu, *J. Power Sources*, 2011, **196**, 2422–2426.
8 Y. Xiao, J. Wu, G. Yue, J. Lin, M. Huang and Z. Lan, *Electrochim. Acta*, 2011, **56**, 8545–8550.

9 K. Li, Y. Luo, Z. Yu, M. Deng, D. Li and Q. Meng, *Electrochem. Commun.*, 2009, **11**, 1346–1349.
10 K. S. Lee, H. K. Lee, D. H. Wang, N.-G. Park, J. Y. Lee, O. O. Park and J. H. Park, *Chem. Commun.*, 2010, **46**, 4505–4507.
11 M. Wu, X. Lin, Y. Wang, L. Wang, W. Guo, D. Qu, X. Peng, A. Hagfeldt, M. Graetzel and T. Ma, *J. Am. Chem. Soc.*, 2012, **134**, 3419–3428.
12 Y. Wang, C. Zhao, D. Qin, M. Wu, W. Liu and T. Ma, *J. Mater. Chem.*, 2012, **22**, 22155–22159.
13 Z. Huang, X. Liu, K. Li, D. Li, Y. Luo, H. Li, W. Song, L. Chen and Q. Meng, *Electrochem. Commun.*, 2007, **9**, 596–598.
14 A. M. Slaney, V. A. Wright, P. J. Meloncelli, K. D. Harris, L. J. West, T. L. Lowary and J. M. Buriak, *ACS Appl. Mater. Interfaces*, 2011, **3**, 1601–1612.
15 M. Wang, A. M. Anghel, B. Marsan, N.-L. Cevey Ha, N. Pootrakulchote, S. M. Zakeeruddin and M. Gratzel, *J. Am. Chem. Soc.*, 2009, **131**, 15976–15977.
16 Y. Wang, M. Wu, X. Lin, Z. Shi, A. Hagfeldt and T. Ma, *J. Mater. Chem.*, 2012, **22**, 4009–4014.